Analysis on signals for LEO-PNT beyond GNSS

Fran Fabra, Daniel Egea-Roca, José A. López-Salcedo and Gonzalo Seco-Granados
Department of Telecommunications and Systems Engineering, IEEC-CERES
Universitat Autònoma de Barcelona
Barcelona, Spain
fabra@ieec.cat

***Abstract*—The utilization of Low Earth Orbit (LEO) platforms for Positioning, Navigation, and Timing (PNT) applications represents an innovative field of research. The increasing interest in this domain is further propelled by the emergence of LEO mega-constellations, signifying a paradigm shift in satellite-based communication and navigation systems. The primary objective of this research is to establish an end-to-end testbed capable of systematically examining diverse signal types in the LEO-PNT context. In doing so, we concentrate on Global Navigation Satellite System (GNSS)-like signals as a benchmark for comparison and explore the pioneering application of Chirp Spread Spectrum (CSS) signals to evaluate their potential for enhancing PNT capabilities. The paper describes the simulation framework and provides the initial results obtained under a case example using the orbital parameters of the Globalstar system.**

***Index Terms*—LEO-PNT, Chirp, CSS, GNSS, open-source**

I. Introduction

The combination of both a democratization of access to space, boosted by the proliferation of low-cost launching systems, and a high demand for Positioning, Navigation, and Timing (PNT) applications with unprecedented performance, has brought attention to the use of low Earth orbit (LEO) platforms as PNT providers with global coverage. Compared to current global navigation satellite systems (GNSSs), the use of lower orbits benefits with better power budgets and higher dynamics, which enables faster decorrelation properties of the measurements [1] [2].

Different types of signals can be considered for satellite-based PNT purposes with their benefits and drawbacks. The first candidate could be based on signals currently employed in GNSS, which are generally referred to as direct-sequence spread spectrum (DSSS). Unfortunately, the high dynamics from LEO transmitters might pose a challenge for both acquisition and tracking in traditional GNSS architectures. However, the strong background in GNSS applications from the research community has already addressed this type of problem when considering users with even higher dynamics so that this experience can be adapted to LEO-PNT. Another alternative is the use of chirp spread spectrum (CSS) signals. Traditionally employed in Radar applications, these signals have a lower complexity in scenarios with a wider Doppler spread than DSSS signals, thus being a suitable option for narrow-band LEO-PNT. Finally, the standardization of 5G and 6G has drawn attention to orthogonal frequency division multiplexing (OFDM) signals for wideband applications. Moreover, user localization and the use of non-terrestrial networks (NTNs) are targeted in this process [3], which are two aspects that being combined, perfectly fit with LEO-PNT.

This activity has been partially supported by the Catalan Government in the framework of the New Space Strategy of Catalonia.

Intending to develop an end-to-end testbed for analyzing the performance in terms of PNT of the different types of signals considered in realistic scenarios, the initial work presented here focuses on the two first categories: GNSS-like and CSS signals. Section II describes (1) the process of extrapolating the signals to a LEO scenario, (2) the modifications done in a GNSS open-source software receiver to support higher dynamics, and (3) the initial steps for building a Chirp-based LEO-PNT receiver. Then, section III provides the results obtained in a case example built using the orbital parameters of the Globalstar system, where the GNSS-like signals are used for validating the end-to-end testbed and the first results from the Chirp signals are shown. It is worth mentioning that the analysis at this point is yet limited to first-order observables: range and Doppler estimation residuals.

II. Simulation framework

A. Signal generation

The equivalent baseband LEO-PNT signal that would be acquired by the receiver is generated by the following:

$$r(t) = \sum_{i=1}^{\#\text{sats}} s_i(t - \delta_i(t)) e^{j(2\pi f_c \delta_i(t) + \phi_i)} + n(t) + \epsilon(t) \quad (1)$$

where i is the index of the different LEO satellites in view, $s_i(t)$ is the transmitted signal at baseband (GNSS-like or Chirp in our analysis), $\delta_i(t)$ is the latency needed to reach the receiver from satellite i, f_c is the carrier frequency of the system, ϕ_i is a random phase offset, $n(t)$ is the noise contribution and $\epsilon(t)$ accounts for the rest of residual unmodeled effects.

Once a baseband signal model is implemented, the most tricky element is the computation of the time series of latency values $\delta_i(t)$. This task is done by means of the "satelliteScenario" tools from MATLAB, which allows to compute the positions and velocities of the different satellites at a given time. The orbital parameters of the desired constellation are injected through a two-line elements (TLE) file, which can be obtained from [6]. Then, an iterative loop is applied that, given a receiver position and time t_{rx}, computes the positions and velocities of all satellites in view at the corresponding time $t_{\text{tx},i}$ that would be required for the signal transmitted to

reach the receiver at $t_{\rm rx}$. The time series of $\delta_i(t)$ obtained are also employed to compute the reference range and Doppler evolutions that will be later used for validation of the results.

As a last comment, it is important to point out that with this procedure it would not be difficult to include additional effects, such as ionospheric and tropospheric delays based on well-known models from the GNSS literature or different multipath components.

B. GNSS software receiver

The software receiver employed for processing GNSS-like signals is a modified version of FGI-GSRx [4]. In addition to including signals with different characteristics than those transmitted from current GNSS, such as frequency band, modulation configuration, code length, rate, etc., the modifications applied have primarily addressed the adaptation of the acquisition and tracking engines to support high dynamics typical from LEO systems.

The most relevant features included are:

- Code Doppler compensation during acquisition.
- Possibility of Doppler and Doppler drift aiding to enable long integration times during acquisition for indoor and low-energy scenarios.
- Inclusion of additional tracking strategies, such as higher-order loops and frequency-aided schemes.
- Smooth state transitions during tracking to enable a more robust adaptation to the narrower loop bandwidth value set at the input configuration (fine tracking state).

This modified version of the software receiver (limited to acquisition and tracking engines) is available at [5].

C. Adaptation of CSS signals

We consider a CSS waveform that linearly varies its frequency in a given bandwidth B during a chirp period $T_{\rm c}$. The rate of variation is defined by the *chirp rate* as $\mu \doteq B/T_{\rm c}$, and the chirp frequency swept is fixed to B by using the modulus-x operator, $[\cdot]_x$, as follows: $f_\mu(t) = [\mu t]_B - B/2 = \mu t_n - B/2$, with $t_n \doteq [t]_{T_{\rm c}} = \{t : 0 \le t < T_{\rm c}\}$. The baseband signal model for the CSS with frequency $f_\mu(t)$ can be written as

$$s_\mu(t) = e^{j\phi_\mu(t)} = e^{j\pi(\mu t_n - B)t_n}, \tag{2}$$

and it corresponds to the up-chirp signal. Down-chirp signals have a negative slope and they correspond to the complex conjugate of the up-chirp, i.e., $s^*_\mu(t)$.

For the joint estimation of time-delay and Doppler frequency with chirp signals, we need the joint transmission of up- and down-chirp components written as $s_\mu(t) + s^*_\mu(t) = 2\cos(\phi_\mu(t))$ and referred as to BOK-chirp signal [9]–[11]. Furthermore, we should consider the transmission of different signals for different satellites. For that, we rely on the multi-dual slope (MDS) scheme introduced in [9], but using the two following slopes for the i-th satellite:

$$\mu_{i,1} = i \cdot (\mu/N_{\rm sat}) \text{ and } \mu_{i,2} = 2\mu - \mu_{i,1}, \tag{3}$$

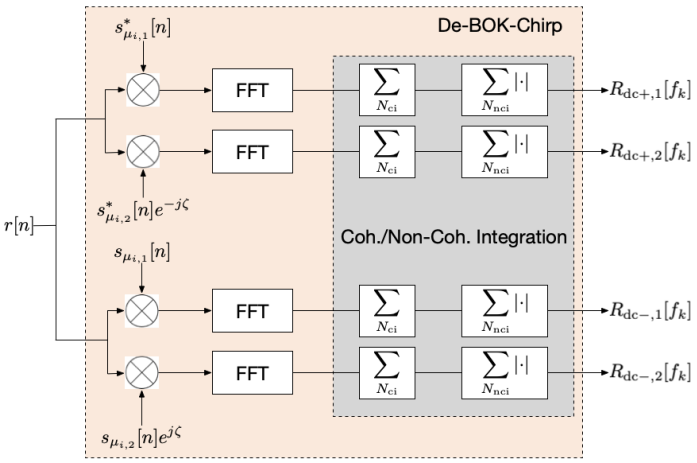

Fig. 1. CSS receiver engine (analogous to GNSS-like correlation).

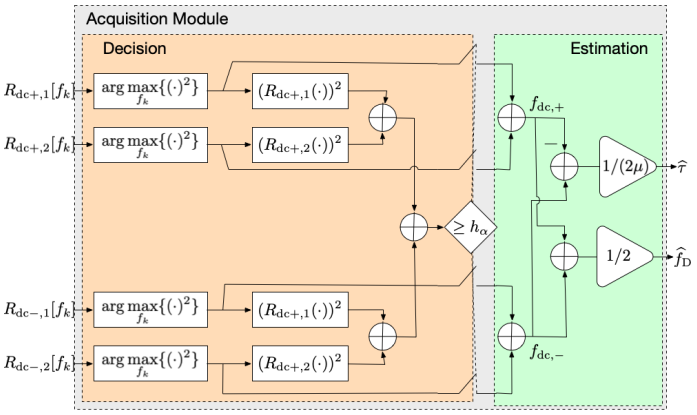

Fig. 2. Acquisition module for the CSS signal.

and the transmission of the following signal with unit power:

$$s_i(t) = \begin{cases} \sqrt{2}\cos\left(\phi_{\mu_{i,1}}(t) + \theta_k\right), & (k-1)T_{\rm c} \le t \le k\frac{T_{\rm c}}{2} \\ \sqrt{2}\cos\left(\phi_{\mu_{i,2}}(t) + \zeta_k\right), & k\frac{T_{\rm c}}{2} < t < kT_{\rm c} \end{cases}, \tag{4}$$

where $\theta_k = (k-1)\pi\phi_{\mu_{i,2}}(T_{\rm c}) + \zeta_1$, and $\zeta_k = \theta_k + \pi\Delta\mu T_{\rm c}/2$ with $\Delta\mu = \mu_{i,1} - \mu_{i,2}$.

Note that $f_\mu(t) \in \pm B/2$, so that each baseband chirp can be sampled at $F_{\rm s} = lB$ producing $N_{\rm c} = lBT_{\rm c}$ samples at each chirp period, with $l \ge 1$. Then, we generate the received signal samples $r[n] = r(t)|_{t=n/F_{\rm s}}$ with $n = 0, 1, \ldots,$ and they are fed to the signal processing module of the CSS receiver shown in Fig. 1. At the receiver side, four local replicas corresponding to the two different slopes of each satellite and their corresponding up- and down-chirp components are generated. This corresponds to $s_{\mu_{i,j}}[n]$ and $s^*_{\mu_{i,j}}[n]$, respectively, with $j = 1, 2$. Then, each local replica is multiplied with the received signal, and its fast Fourier transform (FTT) is taken using $N_{\rm c}$ samples. This process is known as the de-chirp, and the architecture in Fig. 1 will be henceforth referred as to the de-BOK-chirp (DBC).

We have considered the application of coherent and non-coherent integration to produce the outputs $R_{{\rm dc}\pm,j}[f_k]$ cor-

responding to the up- and down-chirp de-chirp for the j-th slope, with $f_k = k/T_c$. It is worth noting that the result of the DBC process is equivalent to the GNSS-like correlation process used to obtain the cross ambiguity function (CAF), which is further used to acquire the signal and estimate the time-delay and Doppler parameters. The acquisition is performed with the module shown in Fig. 2, which consists of finding the peaks (i.e., maximum values) of the different de-chirps, $R_{\mathrm{dc}\pm,j}[f_k]$. Then, if the combination of the four peaks exceeds a certain threshold, h_α, we declare the satellite we are processing is visible. In case the satellite is acquired, we combine the frequency of the peaks for the two different slopes to produce $f_{\mathrm{dc}\pm}$. At this point, it is interesting to see that ideally $f_{\mathrm{dc}\pm} = \pm\mu\tau + f_{\mathrm{D}}$, so that combining these frequencies as shown in Fig. 2 we obtain the time-delay and Doppler estimates.

III. First results based on a case example

A. Description of the scenario

The orbits selected for the LEO scenario are from the Globalstar system, at around 1000 km of altitude. The TLE file employed for the simulation of the constellation was obtained from [6]. The receiver is located at the coordinates of our laboratory at UAB and the starting time is set to 00:00:00 UTC on December 10th, 2023. The duration of the simulation is 10 seconds. The initial satellite visibility of the scenario is displayed in Fig. 3, where the different numbers indicate the satellite identification (ID) inside the constellation.

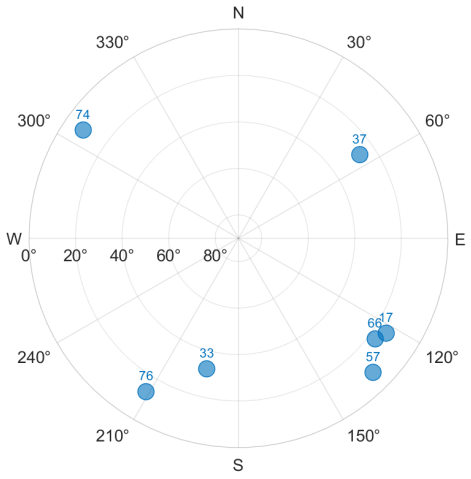

Fig. 3. Satellite visibility under the simulated LEO scenario (the numbers indicate the satellite's ID).

By selecting a carrier frequency of 2.4915 GHz, the dynamics of the different satellites translate into the mean Doppler, Doppler drift, and jerk values given in Table I. As a comparison, the corresponding results typically found in standard GNSS are one, two, and four orders of magnitude lower respectively.

TABLE I
Mean dynamics for the LEO scenario

SatID	Doppler [Hz]	Doppler drift [Hz/s]	Jerk [Hz/s^2]
17	1373	-107.0	0.031
33	34105	-77.0	-0.425
37	-36831	-25.3	0.060
57	12844	-91.0	-0.097
66	3086	-114.6	0.017
74	45467	-9.5	0.064
76	-21257	-57.3	0.096

B. End-to-end validation based on a GNSS-like signal

Given that the modified GNSS software receiver has already been tested in LEO scenarios [7], the use of GNSS-like signals serves as a means for validation of the signal generation process and the results obtained can be employed as a reference for comparison against other signals. For such purpose, a dataless signal has been generated with a binary phase shift keying (BPSK) modulation employing Galileo codes with a length of 4092 chips at a code rate of 8.184 Mcps. The noise power is set such the resultant carrier to noise density (CN0) is 45 dB-Hz for all the cases. This value has been arbitrarily selected as a bottom limit in a LEO-PNT scenario because, although a better power budget is expected when compared against GNSS, international regulations on radiated power could shrink in practice such differential margins for certain frequency bands.

On the receiver side, the signals from all satellites are properly acquired (2 ms of coherent integration). The tracking engine is configured for using a second-order DLL and a third-order PLL aided with a second-order FLL during the whole process. For simplicity, the three loops are configured with the same bandwidth, which takes values of 15 Hz, 7 Hz, and 2 Hz as the engine goes through the three tracking states: pull-in, coarse, and fine tracking. The integration time is set to 0.5 ms (coherent). Figures 4 and 5 provide the results obtained for code-range and Doppler as residuals with respect to the reference model employed during the generation of the transmitted signals. As it can be seen, after the initial fluctuations due to the transition from acquisition to tracking, the receiver can perform a proper estimation of the desired observables.

C. Preliminary results with CSS signals

This section shows the results of processing CSS for PNT transmitted from LEO. To the best of our knowledge, this is the first time this kind of processing has been performed. So, a pioneer open SwRx to process LEO-PNT signals based on CSS is tested. So, the results provided in this section serve as a means for validation of the generated software to process CSS signals transmitted from LEO satellites. A dateless configuration is taken with $T_c = 0.5$ ms and $B = 8.184$ MHz to pose similar properties as the GNSS-like signal used in the previous section. The different satellite slopes are configured from (3) taking $N_{\mathrm{sat}} = 7$. As in the GNSS-like case, the noise

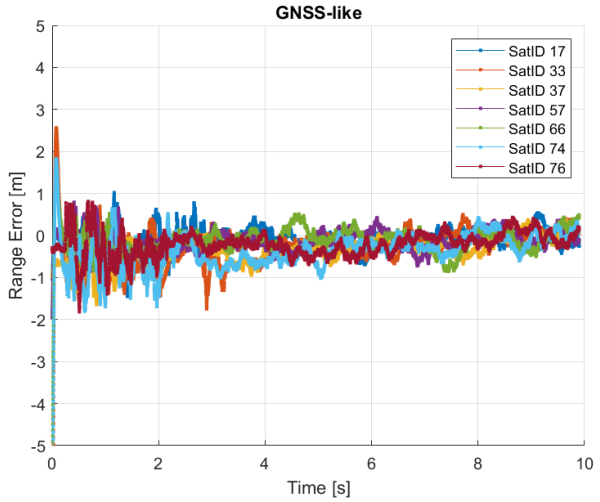

Fig. 4. Range estimation residuals obtained from the GNSS-like signal.

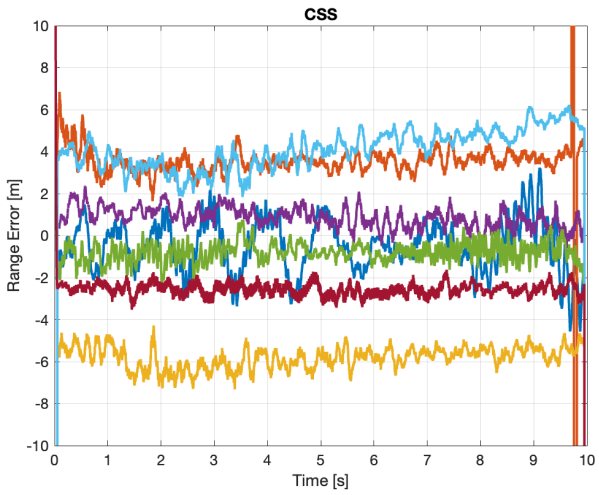

Fig. 6. Range estimation residuals obtained from the CSS signal. Legend from Fig.4 also applies here.

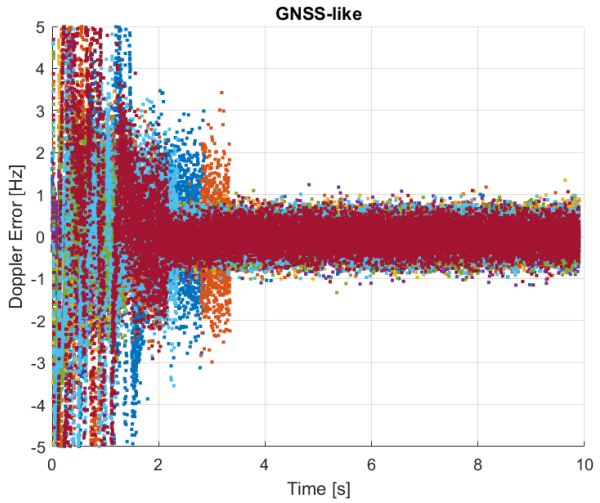

Fig. 5. Doppler estimation residuals obtained from the GNSS-like signal. Legend from Fig.4 also applies here.

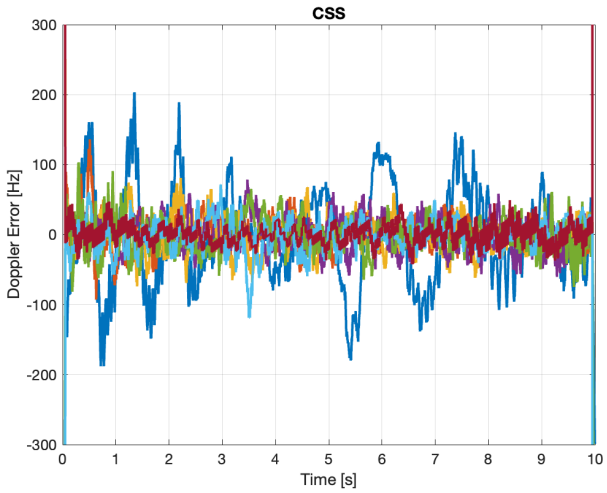

Fig. 7. Doppler estimation residuals obtained from the CSS signal. Legend from Fig.4 also applies here.

power is set such the resultant CN0 is 45 dB-Hz for all the cases.

Although preliminary results with a software receiver are still under development, we see the signals from all the satellites are properly acquired when using 2 ms of coherent integration. An open-loop configuration is employed in order to validate the acquisition module. Better performance is expected when a closed-loop architecture is implemented (under development). The results for the range and Doppler errors (with respect to the reference model) are provided in Fig. 6 and Fig. 7. We see that the receiver can perform the expected estimation we can expect in an open-loop process, where we get range errors on the order of meters and Doppler errors on the order of hundreds of Hz. Therefore, a better performance is expected when a closed-loop architecture is developed.

IV. Discussion

The preliminary results of the CSS give us very valuable insight into the development of a CSS software receiver. For instance, we need to take care of the selection of the slopes used for the MDS scheme, otherwise, we would get coupling between the two slopes of different satellites. This was already highlighted in [9]: to make the MDS work independently of the way we assign the slopes, we need to use $T_c \geq 2\Delta\tau$ with $\Delta\tau$ the maximum time-delay we can experience with the reception from LEO. This has been fixed in this paper by modifying the way we assign the two different slopes for all the satellites (see (3)). Another important point when implementing the DBC for the MDS scheme is that we need to perform a de-chirp process with N_c samples (instead of $N_c/2$) (see Fig. 1). Otherwise, we would get a loss of acquisition for $T_c/2 \leq \tau \leq T_c$. The reason

is that the de-chirp result with $N_c/2$ samples in that case is zero because the chirp part we want to de-chirp is moved to the second (half) part of T_c.

Finally, our purpose is to update our modified version of the GNSS receiver to also work with the new type of signals further developed, given that open-source Software Defined Radio (SDR) solutions, such as many of the examples described in [8] for GNSS, provide a common framework of analysis and discussion, as all internal details and configuration aspects are publicly available.

REFERENCES

[1] L. Ries et al., (2023) "LEO-PNT for Augmenting Europe's Space-based PNT Capabilities," in IEEE/ION Position, Location and Navigation Symposium (PLANS), pp. 329-337. doi: 10.1109/PLANS53410.2023.10139999.

[2] F. S. Prol et al., (2022) "Position, Navigation, and Timing (PNT) Through Low Earth Orbit (LEO) Satellites: A Survey on Current Status, Challenges, and Opportunities," IEEE Access, vol. 10, pp. 83971-84002, doi: 10.1109/ACCESS.2022.3194050.

[3] Dureppagari, H. K. et al. (2023) "NTN-based 6G Localization: Vision, Role of LEOs, and Open Problems." Available at: https://arxiv.org/abs/2305.12259v2

[4] FGI-GSRx Software Receiver. Available online: https://github.com/nlsfi/FGI-GSRx

[5] FGI-GSRx for LEO-PNT. Available online: https://gitlab.com/spcomnav_public/fgi-gsrx-leo-pnt

[6] Celestrak: NORAD GP Element Sets. Available online: https://celestrak.org/NORAD/elements/

[7] F. Fabra, J. A. Lopez-Salcedo, G. Seco-Granados, "Analysis on baseband algorithms for LEO PNT", Proc. European Navigation Conference (ENC), Jun 02, 2023.

[8] T. Pany et al., "GNSS Software-Defined Radio: History, Current Developments, and Standardization Efforts", NAVIGATION: Journal of the Institute of Navigation, Mar 2024, 71 (1) navi.628; DOI: 10.33012/navi.628

[9] D. Egea-Roca, J. A. López-Salcedo, G. Seco-Granados, and E. Falletti, "Comparison of several signal designs based on chirp spread spectrum (CSS) modulation for a LEO PNT system," in Proc. 34th International Technical Meeting of the Satellite Division of the Institute of Navigation (ION GNSS+), 2021, pp. 2804–2818.

[10] D. Egea-Roca, J. Lopez-Salcedo, G. Seco-Granados, and E. Falletti, "Performance analysis of a multi-slope chirp spread spectrum signal for PNT in a LEO constellation," in Proc. 10th IEEE Workshop on Satellite Navigation Technology (NAVITEC), 2022.

[11] D. Egea-Roca, J. A. López-Salcedo, and G. Seco-Granados, "Performance analysis of the pilot- and data-component of a CSS signal for LEO-PNT," Eng. Proc., vol. 54, no. 1, p. 35, 2023.